Supporting information

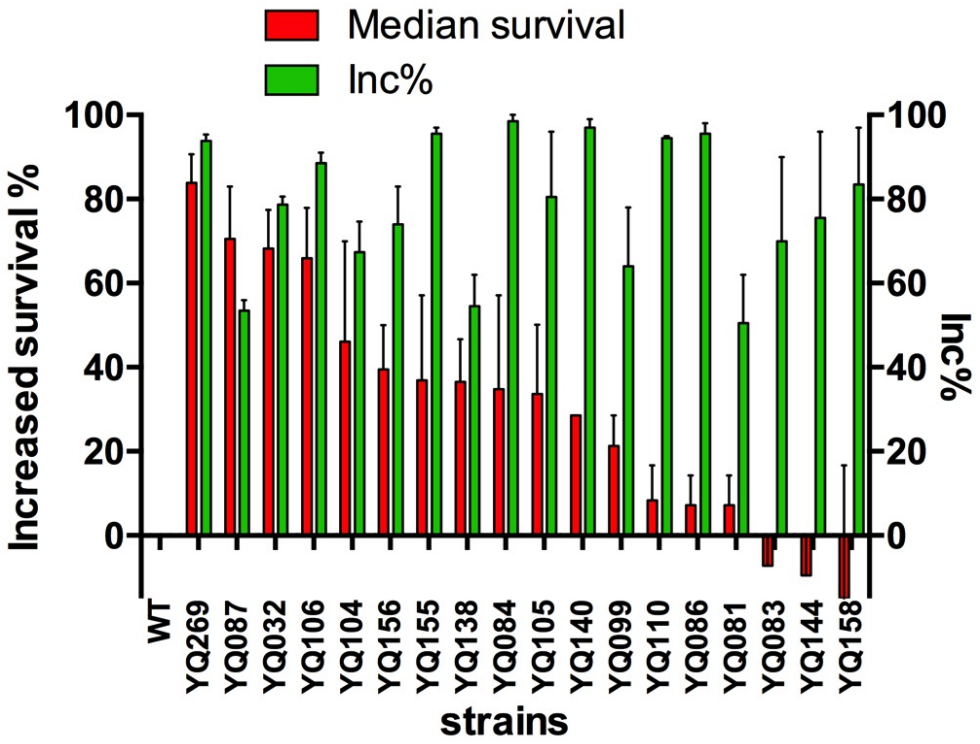

Figure S1. The Inc percentage and increased survival percentage of EMS-induced alleles. The ratio of the enhanced GFP expression signals in the intestine of these 18 mutant worms were reconfirmed by feeding with GFP-labeled EHEC for 24 h at 20°C. The susceptibility of these 18 mutants to EHEC was examined and the increased percentage of median survival days was compared to that of wild-type N2.

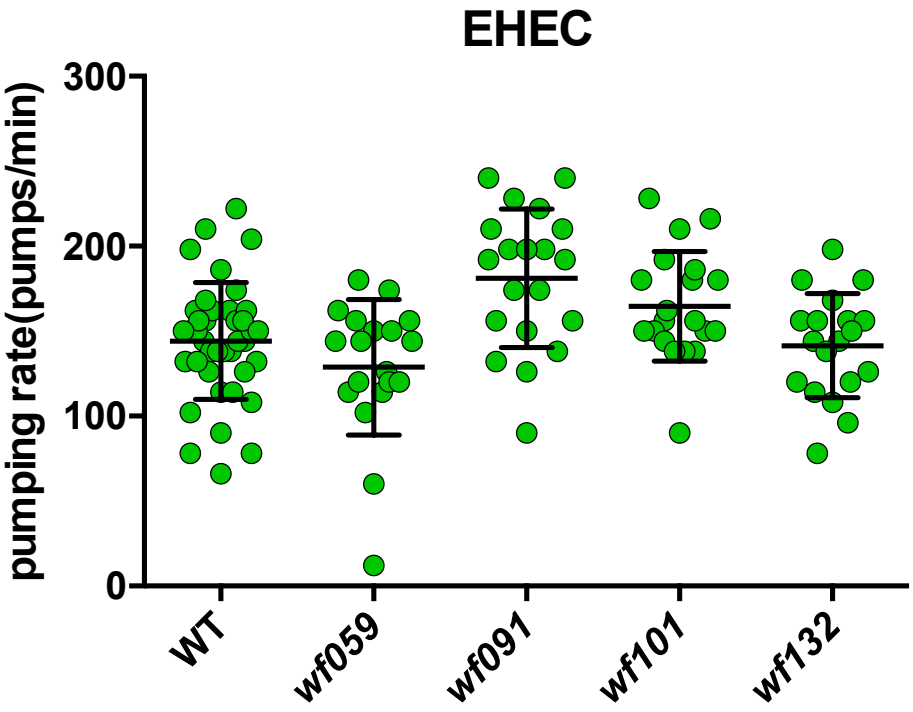

Figure S2. Four *inc* mutants display comparable pumping rate to WT.

The pharyngeal pumping rate of wild-type (WT) N2 animals and the four *inc* mutants, *wf059*, *wf091*, *wf101*, and *wf132* fed on EHEC for one day at 20°C. The pumping rate between N2 animals and the four *inc* mutants was not significantly increased compared to the unpaired t-test.

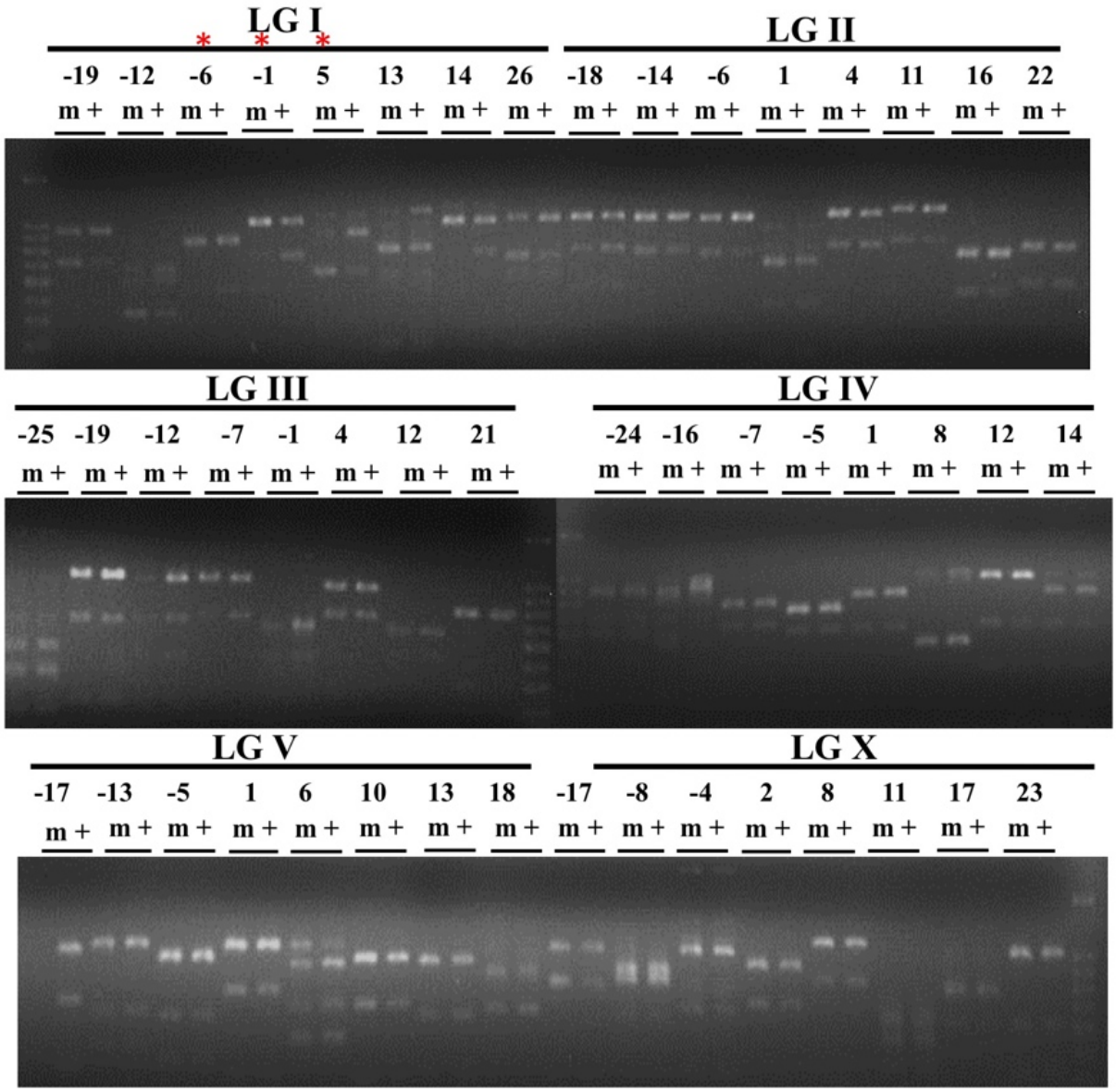

Figure S3. SNP mapping of *inc-1(wf132)*. Chromosome mapping of *inc-1(wf132)*. Each pair of lanes shows results from the SNP at the indicated genetic map position, using either the mutant (m) or the non-mutant (+) template. Linkage is visible as an increase in the proportion of Bristol N2 DNA in mutant lanes compared to the non-mutant lanes, and is visible on LG I from -6 to +5.

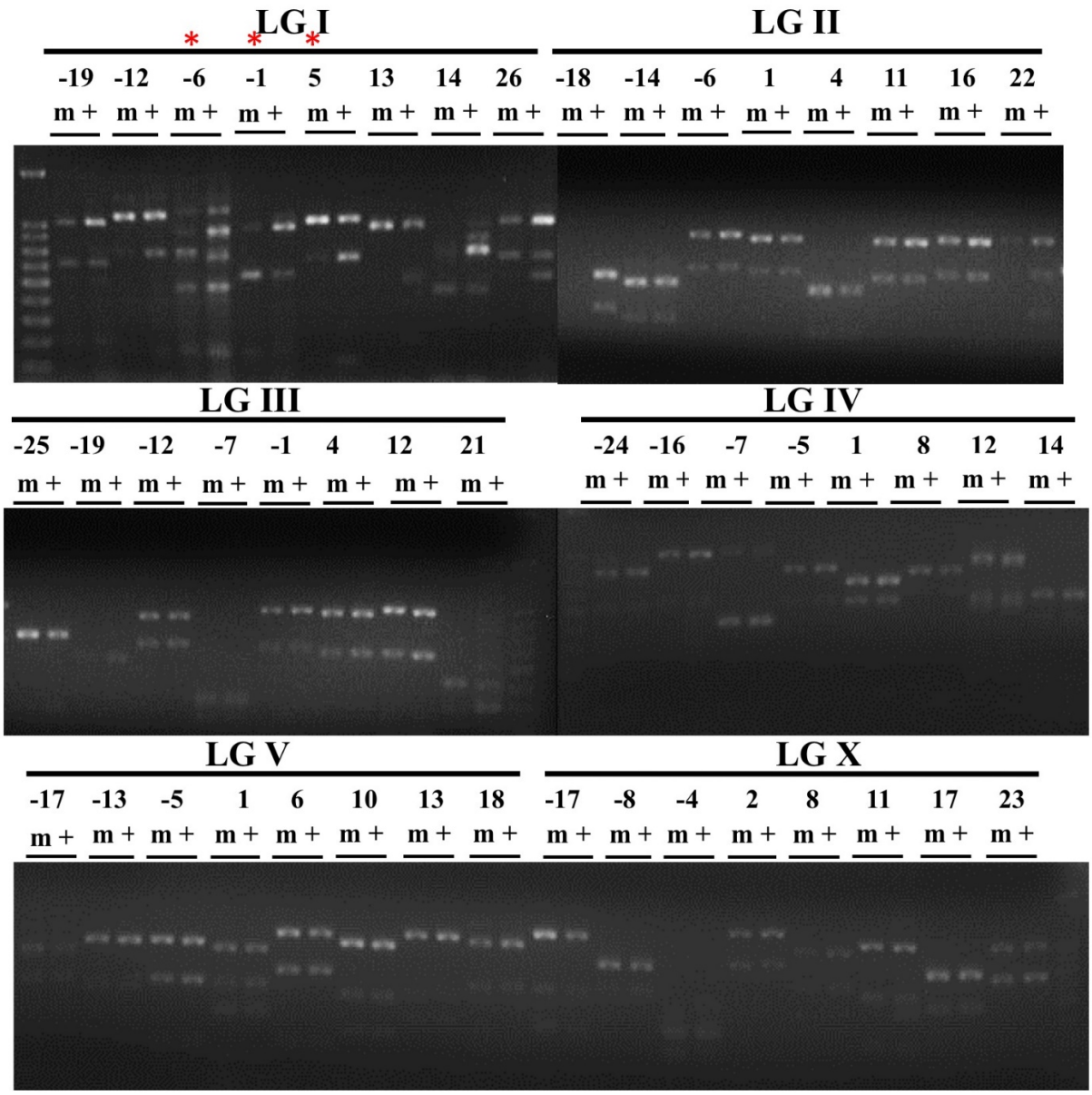

Figure S4. SNP mapping of *inc-1(wf059)*. Chromosome mapping of *inc-1(wf059)*. Each pair of lanes shows results from the SNP at the indicated genetic map position, using either the mutant (m) or the non-mutant (+) template. Linkage is visible as an increase in the proportion of Bristol N2 DNA in mutant lanes compared to the non-mutant lanes, and is visible on LG I from -6 to +5.

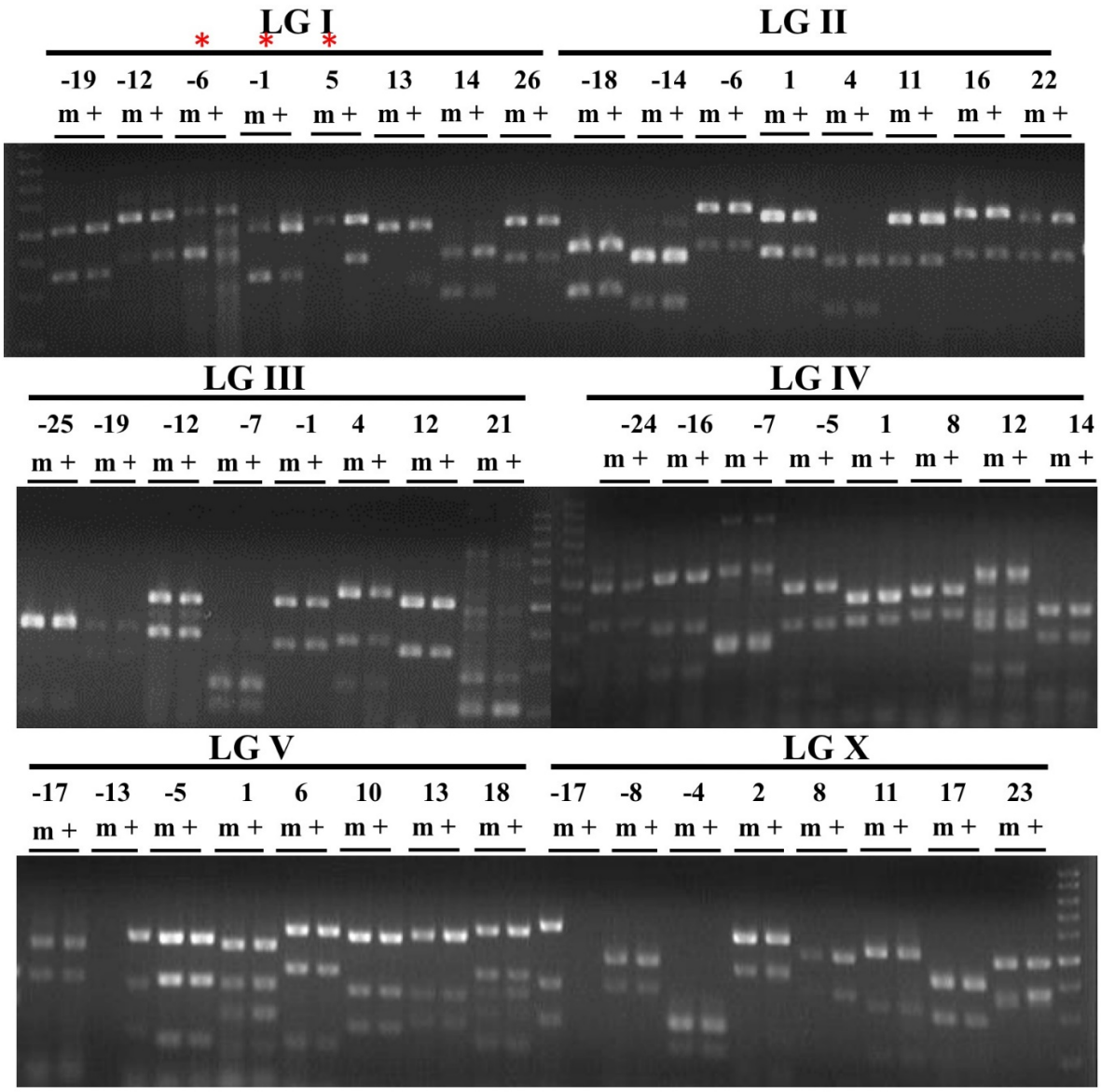

Figure S5. SNP mapping of *inc-1(wf101)*. Chromosome mapping of *inc-1(wf101)*. Each pair of lanes shows results from the SNP at the indicated genetic map position, using either the mutant (m) or the non-mutant (+) template. Linkage is visible as an increase in the proportion of Bristol N2 DNA in mutant lanes compared to the non-mutant lanes, and is visible on LG I from -6 to +5.

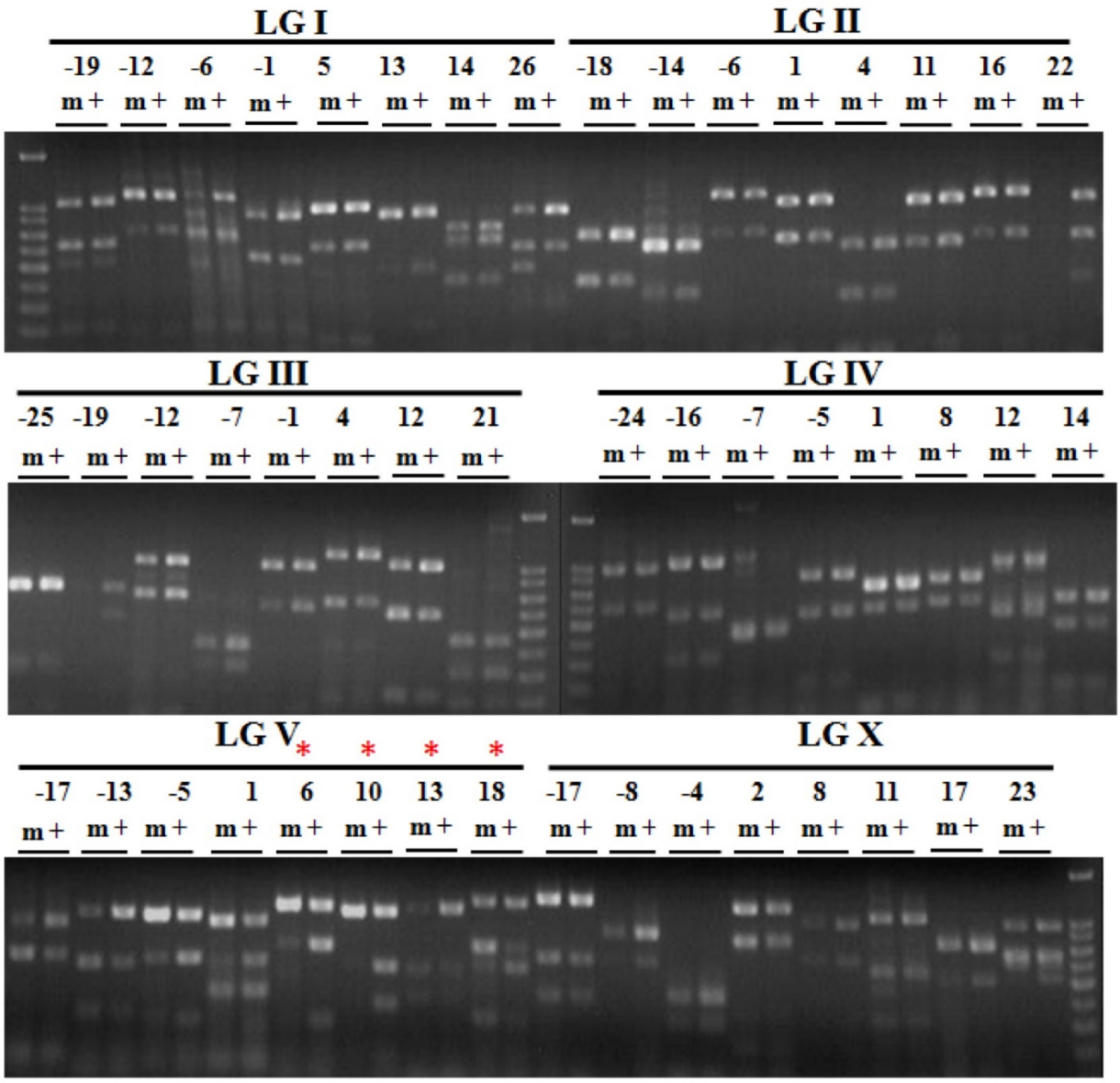

Figure S6. SNP mapping of *inc-2(wf091)*. Chromosome mapping of *inc-2(wf091)*. Each pair of lanes shows results from the SNP at the indicated genetic map position, using either the mutant (m) or the non-mutant (+) template. Linkage is visible as an increase in the proportion of Bristol N2 DNA in mutant lanes compared to the non-mutant lanes, and is visible on LG V from +6 to +18.

LG I: W03D8(-6)

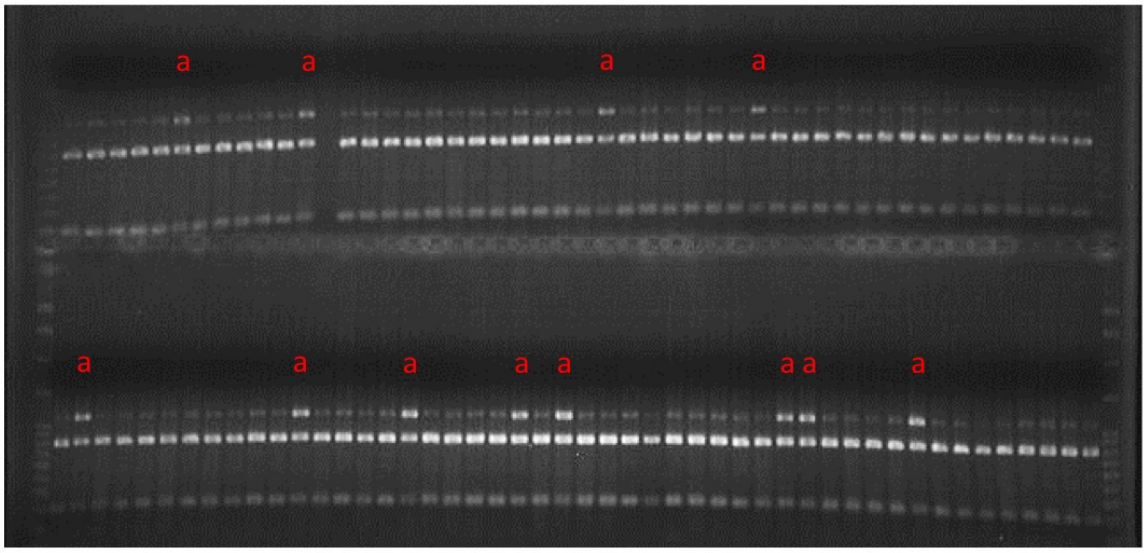

LG I: D1007(-1)

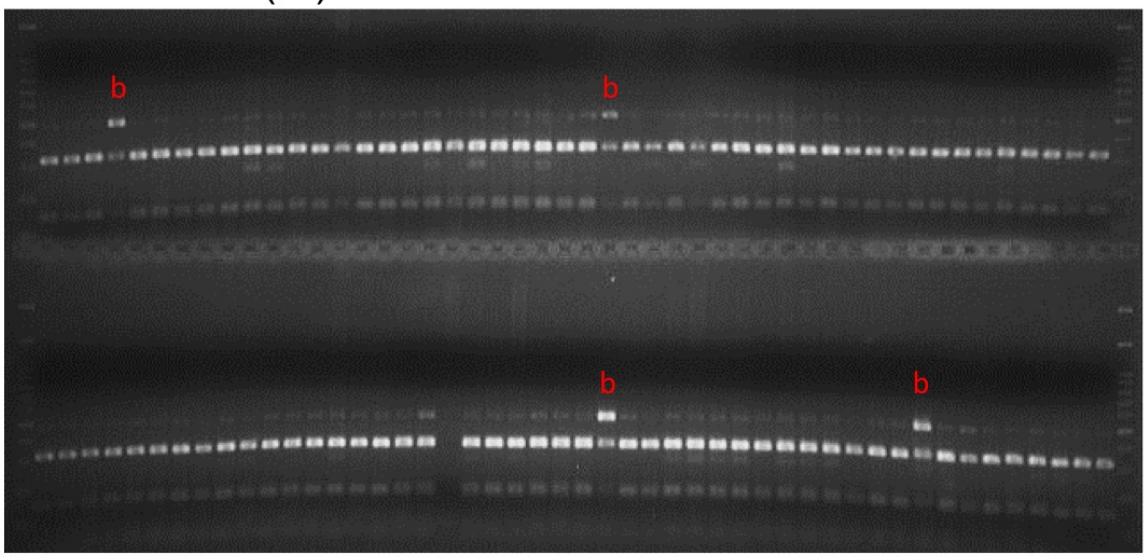

LG I: B0205(+5)

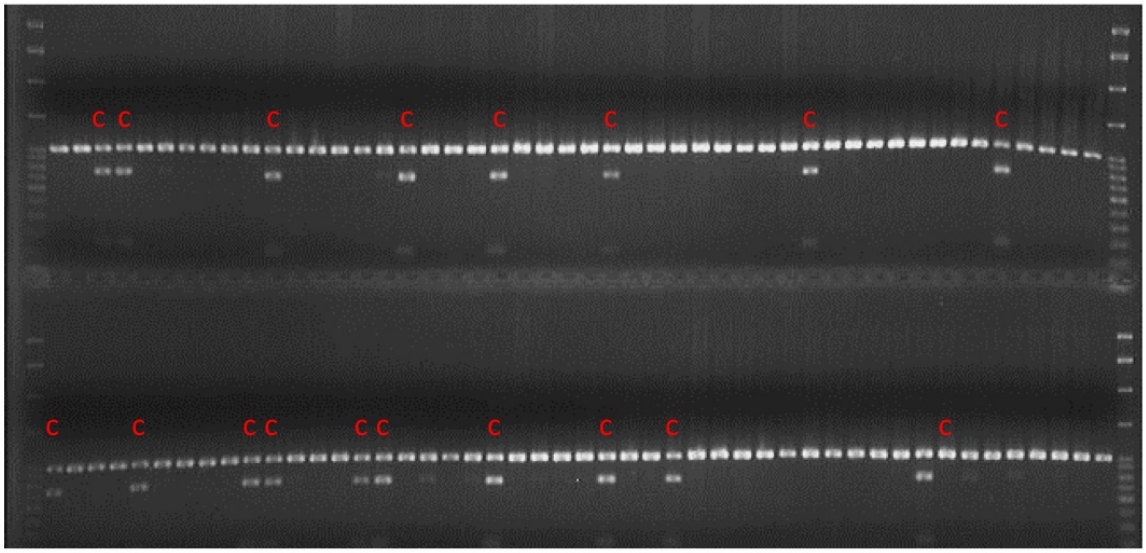

Figure S7. SNP mapping of *inc-1(wf132)*. Interval mapping of *inc-1(wf132)*. Each column is an individual mutant recombinant, assayed for the three SNPs W03D8 (top row), D1007 (second row) and B0205 (bottom row). Most (40/96) recombinants show Bristol DNA at all four SNPs. This indicates that these recombinants were homozygous Bristol at these loci, as expected for tightly linked markers. Fifty-six animals show half Bristol and half Hawaiian DNA at one or more loci, indicating that they have one chromosome that is recombinant in this interval. Columns marked "a" are recombinant in the W03D8 interval, those marked "b" in the W03D8-D1007 interval, those marked "c" in the D1007- B0205 interval.

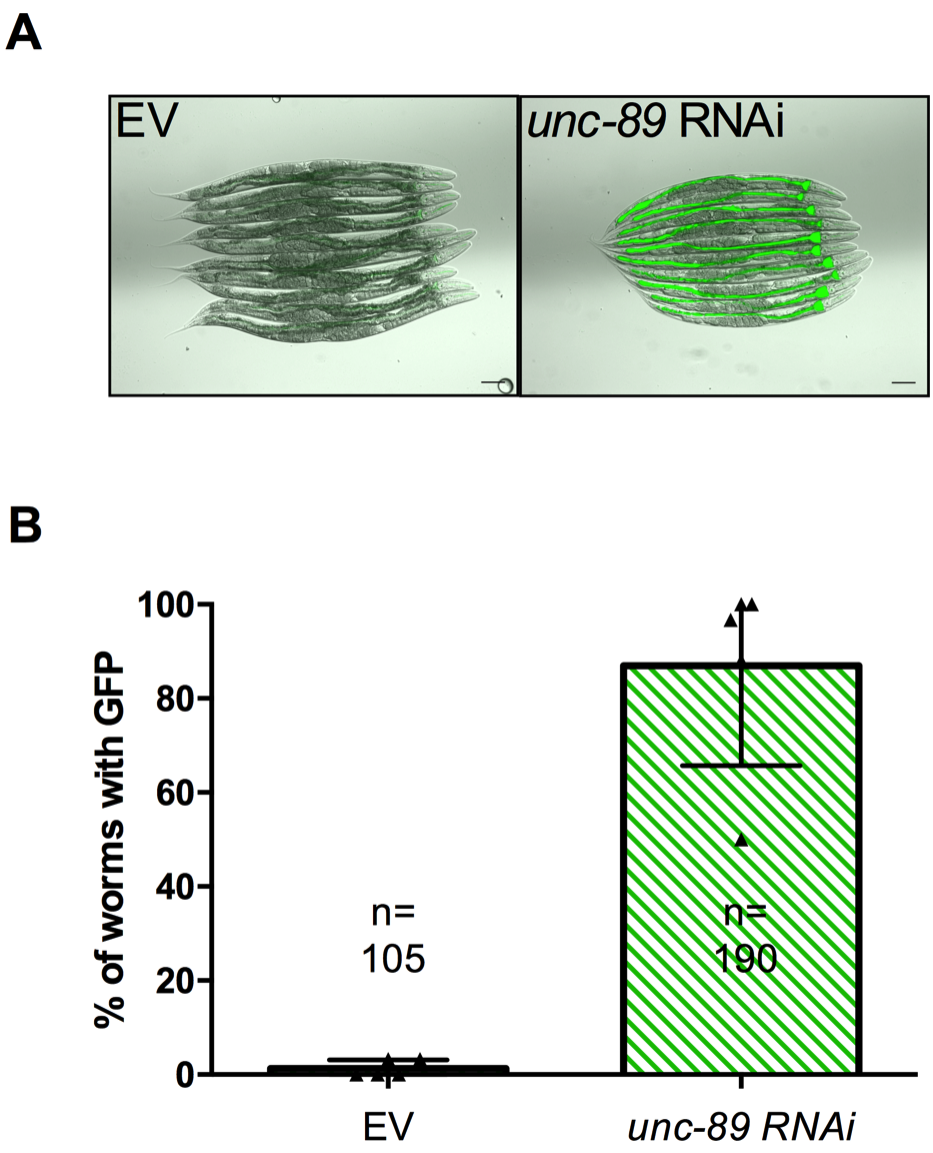

Figure S8. RNAi knockdown of *unc-89* confers Inc. (A) The representative images of *unc-89* RNAi animals exhibiting Inc are shown. Animals were treated with EHEC-GFP for one day and the GFP signal expression was monitored in the intestinal lumen. The scale bar indicates 100 μm. **(B)** RNAi knockdown of *unc-89* in *rrf-3(pk1426)* demonstrated a significantly increased percentage of Inc compared to the empty vector (EV) control while feeding EHEC-GFP for one day. Error bars indicate the standard deviation (SD). The total numbers of animals tested in each group are indicated by n.

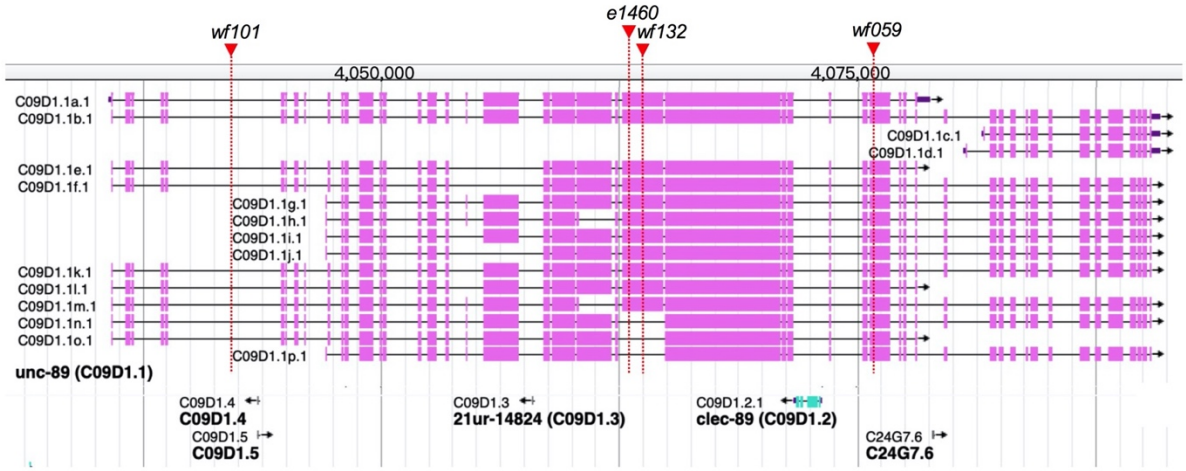

Figure S9. Diagram of different *unc-89* isoforms and the mutation loci of *e1460, wf059, wf101* and *wf132* alleles. *e1460* mutation changes cytosine (C) to thymine (T). *wf059* mutation also changes cytosine (C) to thymine (T). *wf101* allele contains a two guanine (G) deletion at 6,408 to 6,409 nt in the intron. *wf132* mutation changes guanine (G) to adenine (A). Image were adapted from wormbase (https://www.wormbase.org/).

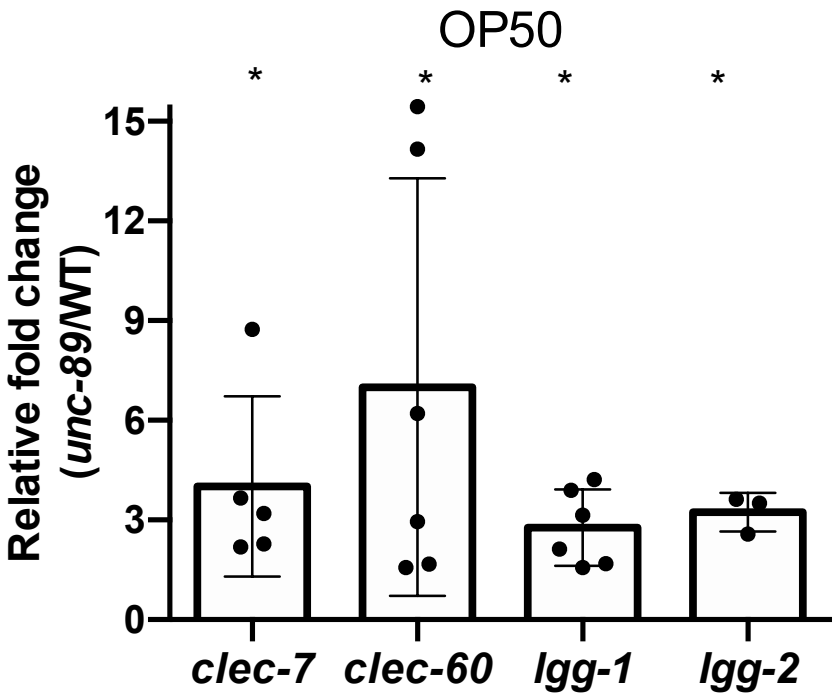

Figure S10. qRT-PCR analysis of the expression of *clec-7*, *clec-60*, *lgg-1* and *lgg-2*. cDNA from wild-type and *unc-89* mutant animals feeding on OP50 for 24 hours at 20°C were analyzed. Results were normalized to the expression level of the *eft-2* control gene. Expression is relative to wild-type N2 animals. *, $P < 0.05$ compared to the control group by the unpaired t-test. Error bars represent SD.

Table S1. Bacterial and nematode strains and plasmids used for this study

Strains or plasmids	Relevant characteristic(s)	Source or Reference
Bacterial strains		
OP50	Standard laboratory food source	(BRENNER 1974)
EDL933	*E. coli* O157:H7 isolated from raw hamburger meat implicated in hemorrhagic colitis outbreak	(STROCKBINE *et al.* 1986)
EDL933-GFP	*E. coli* O157:H7 EDL933 transformed with pFPV25.1;Am^r	(CHOU *et al.* 2013)
OP50-GFP	*E. coli* OP50 transformed with pFPV25.1;Am^r	(CHOU *et al.* 2013)
***C. elegans* strains**		
N2	*C. elegans* wild type	(BRENNER 1974)
YQ032	*inc-1(wf059)*	This study
YQ087	*inc-2(wf091)*	This study
YQ106	*inc-1(wf101)*	This study
YQ139	*inc-1(wf132)*	This study
YQ268	*inc-1(wf132);dpy-5(e61)*	This study
YQ269	*wf132; backcrossed* to wild-type N2 four times	This study
GK454	*unc-119,dkIs247[Pact-5::mCherry::HA::act-5, unc119(+)]*	(SATO *et al.* 2011)
MT464	*unc-5(e53); dpy-11(e224); lon-2(e678)*	CGC
MT465	*dpy-5(e61);bli-2(e768);unc-32(e189)*	CGC
DR293	*dpy-5(e61);unc-101(m1)*	CGC
CB0061	*dpy-5(e61)*	CGC
CB73	*unc-15(e73)*	CGC
CB190	*unc-54(e190)*	CGC
CB767	*bli-3(e767)*	CGC
CB128	*dpy-10(e128)*	CGC
CB1	*dpy-1(e1)*	CGC
CB12	*dpy-9(e12)*	CGC
CB224	*dpy-11(e224)*	CGC

CB4123	*lon-3(e2175)*	CGC
CB1460	*unc-89(e1460)*	CGC
RW85	*unc-89(st85)*	CGC
CB4856	Wild type isolated from a pineapple field in Hawaii in 1972	CGC
DA597	*phm-2(ad597)*	CGC
NL2099	*rrf-3(pk1426)*	CGC
IK575	*ttx-7(nj40)*	CGC
EL329	*ego-1(om58)/hT2 [dpy-18(h662)]; +/hT2 [bli-4(e937)]*	CGC
EJ420	*gon-2(dx23);fer-1(hc1)*	CGC
PR671	*tax-2(p671)*	CGC
RB1722	*T08G11.1(ok2190)*	CGC
GR1321	*tph-1(mg280);cam-1(vs166)*	CGC
YQ528	*unc-89(wf132);tph-1(mg280)*	This study
YQ530	*unc-89(wf132).* F2 progeny segregated from YQ269 and GR1321 cross parents.	This study
YQ531	*tph-1(mg280).* F2 progeny segregated from YQ269 and GR1321 cross parents.	This study
OP433	*unc119(tm4063);wgIs433[hlh-30::TY1::EGFP::3xFLAG+unc-119(+))]*	CGC
JIN1375	*hlh-30(tm1978)*	CGC
YQ493	*unc-89(e1460);hlh-30(tm1978)*	This study
YQ502	*unc-89;unc119(tm4063);wgIs433[hlh-30::TY1::EGFP::3xFLAG+unc-119(+))]*	This study

CGC represent *Caenorhabditis* Genetics Center.

Table S2. Potential gene candidates for *wf132* predicted from WGS analysis.

Position (cM)	Gene_ID	Gene name
-1.73	C09D1.1	*unc-89*
-1.04	D1007.3	*D1007.3*
0.74	C27A12.9	*C27A12.9*
1.16	C55B7.9	*mdt-18*
1.32	E02D9.1	*E02D9.1*
1.88	F13G3.5	*ttx-7*
2.21	F26A3.3	*ego-1*
2.95	T01H8.5	*gon-2*
3.22	F29D10.1	*F29D10.1*
3.3	T08G11.1	*T08G11.1*
3.41	F36F2.5	*tax-2*

References

Brenner, S., 1974 The genetics of Caenorhabditis elegans. Genetics 77**:** 71-94.

Chou, T. C., H. C. Chiu, C. J. Kuo, C. M. Wu, W. J. Syu *et al.*, 2013 Enterohaemorrhagic Escherichia coli O157:H7 Shiga-like toxin 1 is required for full pathogenicity and activation of the p38 mitogen-activated protein kinase pathway in Caenorhabditis elegans. Cell Microbiol 15**:** 82-97.

Sato, M., K. Saegusa, K. Sato, T. Hara, A. Harada *et al.*, 2011 Caenorhabditis elegans SNAP-29 is required for organellar integrity of the endomembrane system and general exocytosis in intestinal epithelial cells. Molecular biology of the cell 22**:** 2579-2587.

Strockbine, N. A., L. Marques, J. W. Newland, H. W. Smith, R. K. Holmes *et al.*, 1986 Two toxin-converting phages from Escherichia coli O157: H7 strain 933 encode antigenically distinct toxins with similar biologic activities. Infection and immunity 53**:** 135-140.